NANO LETTERS

LETTER

pubs.acs.org/NanoLett

Three-Dimensional GaN/AlN Nanowire Heterostructures by Separating Nucleation and Growth Processes

Santino D. Carnevale,[†] Jing Yang,[†] Patrick J. Phillips,[†] Michael J. Mills,[†] and Roberto C. Myers*[,†,‡]

[†]Department of Materials Science and [‡]Engineering and Department of Electrical and Computer Engineering, The Ohio State University, Columbus, Ohio 43210, United States

ABSTRACT: Bottom-up nanostructure assembly has been a central theme of materials synthesis over the past few decades. Semiconductor quantum dots and nanowires provide additional degrees of freedom for charge confinement, strain engineering, and surface sensitivity—properties that are useful to a wide range of solid state optical and electronic technologies. A central challenge is to understand and manipulate nanostructure assembly to reproducibly generate emergent structures with the desired properties. However, progress is hampered due to the interdependence of nucleation and growth phenomena. Here we show that by dynamically adjusting the growth kinetics, it is possible to separate the nucleation and growth processes in spontaneously formed GaN nanowires using a two-step molecular beam epitaxy technique. First, a growth phase diagram for these nanowires is systematically developed, which allows for control of nanowire density over three orders of magnitude. Next, we show that by first nucleating nanowires at a low temperature and then growing them at a higher temperature, height and density can be independently selected while maintaining the target density over long growth times. GaN nanowires prepared using this two-step procedure are overgrown with three-dimensionally layered and topologically complex heterostructures of (GaN/AlN). By adjusting the growth temperature in the second growth step either vertical or coaxial nanowire superlattices can be formed. These results indicate that a two-step method allows access to a variety of kinetics at which nanowire nucleation and adatom mobility are adjustable.

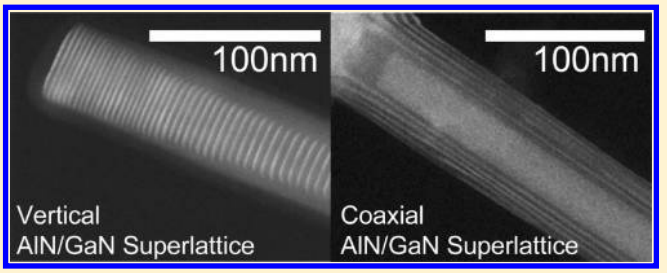

KEYWORDS: Nanostructures, nanowires, nucleation and growth, nitrides, molecular beam epitaxy

Nanowire (NW) heterostructures are attractive for use in semiconductor devices because strain accommodation allows the combination of materials with large lattice mismatch without generating dislocations,[1] structures that are not generally feasible in epitaxial films. In particular, the nanowire heterostructures constructed from the III−N semiconductors (GaN, AlN, and InN) exhibit direct band gaps over a large portion of the electromagnetic spectrum (6.2 eV in AlN to 0.7 in InN) making such NWs especially desirable for optoelectronic applications.[2−5] III−N nanowires grown by plasma-assisted molecular beam epitaxy (PAMBE) can be grown without the use of a catalyst[6] leading to improved electronic and optical performance,[7] unlike NWs grown by the vapor−liquid−solid method. Individual III-nitride NWs can be grown directly on Si wafers[7,8] and consist of material that is nearly defect-free.[8,9]

Catalyst-free GaN NWs begin, as any crystallite does, by first nucleating to a critical size, and then growing.[10] During the nucleation step, GaN islands form and increase in size until they reach a critical radius, after which they grow vertically due to preferential incorporation of adatoms on the c-plane top versus m-plane sidewall.[11,12] Average radius, density, and height can be manipulated by adjusting growth conditions.[7,19,12−15] GaN NWs can be formed by initially depositing an AlN buffer on top of bare Si(111) and then proceeding with GaN deposition.[10,11,14,16] Density can be controlled using an AlN or GaN buffer,[14,17,18] however the buffers are defective.[18]

Previous studies have performed NW growth under static conditions, which limits control over the assembly process. Here we describe a dynamic process that allows synthesis of GaN nanowires with a targeted size and density. First, the density of GaN NWs grown directly on Si(111) substrates is related to the III/V flux ratio and substrate temperature. This provides a system independent parameter space for reproducible growth of NWs of a target density. Next, by adjusting substrate temperature at a specific time during growth, the NW nucleation process is halted. This two-step growth method makes it possible to have independent control of NW density and height, while keeping the average radius of NWs constant. By using this dynamic method, growth kinetics are actively tailored to control adatom mobility and growth anisotropy, allowing for enhancement of vertical (*c*-plane) or coaxial (*m*-plane) growth of GaN for systematic design of three-dimensional nanowire quantum structures.

All samples in this work are grown using a Veeco 930 PAMBE system[19] on n-type Si(111) substrates. Standard effusion cells are

Received: December 7, 2010
Revised: January 10, 2011
Published: January 25, 2011

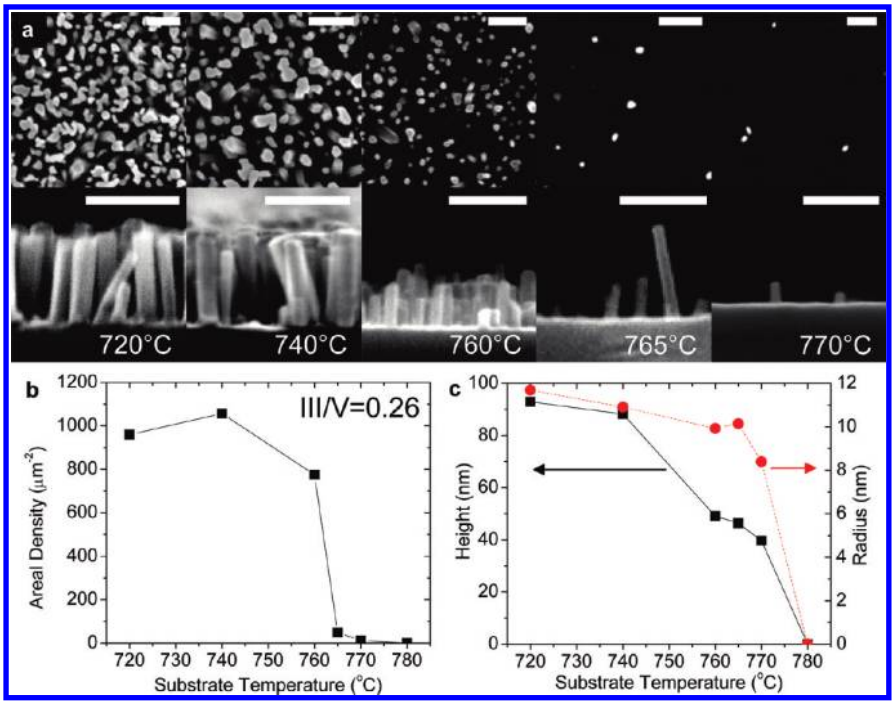

Figure 1. Temperature dependence of GaN nanowire properties. All samples grown with III/V flux ratio = 0.26. (a) Plan view (top) and cross-sectional view (bottom) SEM images at different substrate temperatures labeled in figure. Scale bars are 100 nm. (b) Areal density and (c) average height and radius as a function of substrate temperature. Lines guide the eye.

used for the Ga and Al sources. Active nitrogen is supplied by a Veeco radio frequency plasma source. Beam fluxes are measured using a nude ion gauge at the substrate position. Before growth, the native oxide is removed by heating the substrate to 1000 °C, which is characterized by the appearance of a streaky 1 × 1 reflection high energy electron diffraction (RHEED) pattern out of a diffuse background. Upon cooling, the 1 × 1 changes to a 7 × 7 pattern at 830 °C,[20,21] which is used to calibrate the infrared pyrometer used to measure the substrate temperature. The plasma source is operated at 350 W using a constant N_2 flow rate supplied by a mass flow controller resulting in a N-limited growth rate of 5.1 nm/min for all samples. Preliminary studies show that the Si surface becomes nitridated once the N plasma is lit forming amorphous Si_3N_4 on the surface as evidenced by the disappearance of 7 × 7 pattern into a diffuse background. This occurs even when the nitrogen shutter is closed. To minimize this unintentional nitridation, which is known to occur due to plasma leaking around the shutter, all samples discussed here are grown with the substrate first pointed 180° from the N source during which time the plasma is lit. This minimizes unintentional nitridation as evidenced by the preservation of the 7 × 7 pattern after the substrate is rotated to face the sources and just before the Ga and N shutters are opened. All samples are prepared without use of an AlN buffer layer.

To provide an accurate measure of the III/V flux ratio, a series of samples are grown using a variety of Ga fluxes and a constant supply of active N (constant N_2 background pressure) at substrate temperatures of 720 °C. Cross-sectional scanning electron microscopy (SEM) on each sample determined the thickness, and therefore GaN growth rate at each Ga flux. For low Ga fluxes, the growth rate is linear with Ga flux, denoting the Ga-limited (N-rich, III/V < 1) growth regime. For high Ga fluxes, the growth rate is constant, denoting the N-limited (Ga-rich, III/V >1) growth regime. The Ga flux at which these growth rates intersect is the stoichiometric point (III/V = 1), which is used as a reference point to convert Ga fluxes to equivalent III/V (i.e., Ga to N) ratios.[22]

SEM images along with image analysis software[23] are used to determine nanowire density, height, and radius. All images are obtained on an FEI Sirion scanning electron microscope operating at an accelerating voltage of 15 kV using the "in lens" secondary electron detector. Plan view SEM images allow determination of the NW density and average radius by measuring the area of each NW top and approximating NW tops as circles. NW height is measured directly from cross-sectional SEM images.

Figure 1a displays both plan view (top) and cross-sectional (bottom) SEM images from GaN NW samples grown for 30 min at various substrate temperatures (substrate temperature increases from left to right) at a constant III/V = 0.26. A thousand-fold change in NW areal density (number of NWs per area) due to substrate temperature is apparent. At low temperatures, NW density is roughly constant, and as substrate temperature increases beyond the decomposition temperature of GaN (750 °C),[24,25] density sharply decreases (Figure 1b). The same decrease is seen in both average NW height and radius (Figure 1c) although these are not as strongly affected as density.

To build up a system independent growth phase diagram, 22 samples are grown at various combinations of III/V and substrate temperature (Figure 2). Clearly both substrate temperature and III/V flux ratio have a strong impact on the NW characteristics. A growth window for high density samples exists from 720 to 740 °C for III/V = 0.3 to 0.6. Under these conditions the samples approach a saturation density of approximately 1000 μm^{-2}, which is roughly equal to the saturation density (1000−2000 μm^{-2} for NWs of this size range). At temperatures above 750 °C, density tends to drop, consistent with the onset of thermal decomposition of GaN at these temperatures. The equivalent

dx.doi.org/10.1021/nl104265u |*Nano Lett.* 2011, 11, 866–871

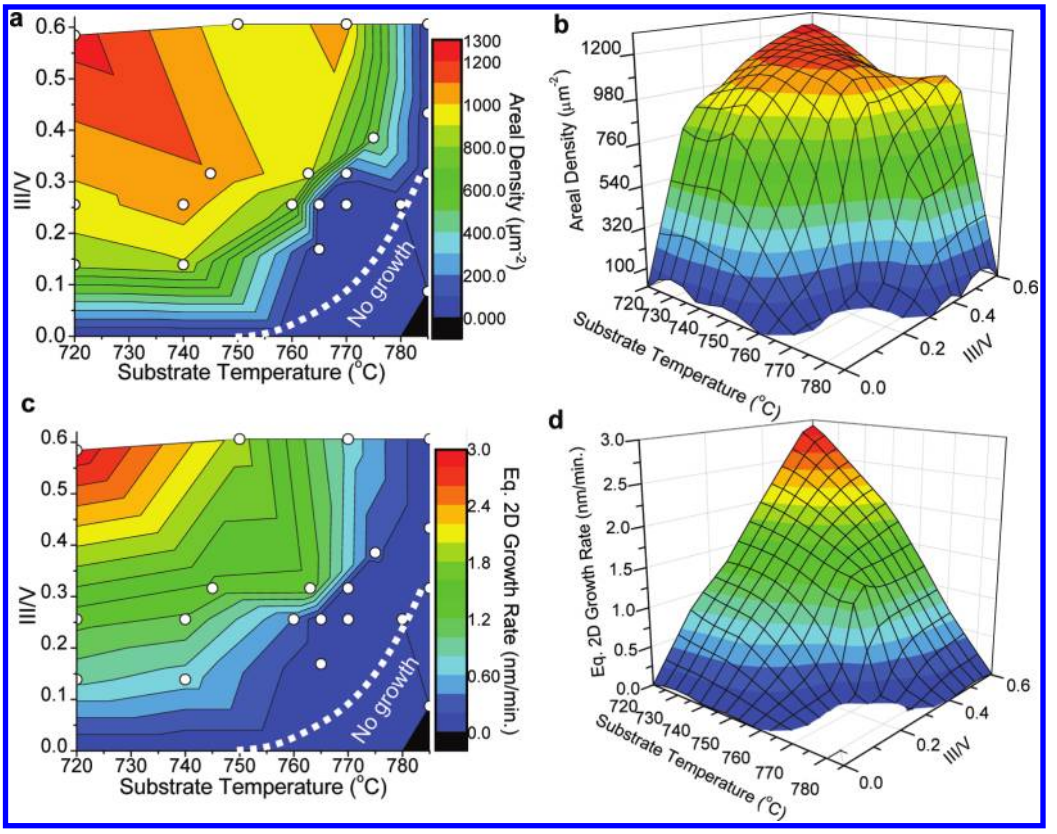

Figure 2. System independent growth phase diagram for catalyst-free GaN nanowires on Si(111). All samples are grown for 30 min. (a) Nanowire areal density as a function of calibrated III/V flux ratio and substrate temperature. Circles denote data points representing actual sample growths. (b) Contour plot of the same data in (a). (c,d) Equivalent two-dimensional growth rate as a function of III/V flux ratio and substrate temperature.

two-dimensional growth rate, calculated by taking the product of average NW volume and areal density divided by deposition time (Figure 2c,d), clearly reveals the "no growth" region due to the decomposition rate exceeding deposition rate. At very low III/V ratios, the NWs cannot form since the decomposition rate exceeds the growth rate (Figure 2c). At high III/V ratios, however, the GaN growth rate can exceed the decomposition rate such that NW nucleation and growth will occur. At intermediate values, various average NW growth rates and densities are attainable. Because all the samples plotted in Figure 2 are grown for 30 min, these growth maps provide a snapshot in time of the nucleation and growth process. Using this information, one can tune NW density, average radius, and height by adjusting substrate temperature and III/V flux ratio. However, these properties are not independently tunable. The challenge is that new NWs continue to nucleate while the previously generated ones are already growing. Thus it is not possible to grow NWs of an arbitrary length while maintaining a low density, as all samples inevitably will reach their saturation density at long enough growth times.

To overcome this limitation, we separate the nanowire nucleation and growth processes into two growth steps. For all of the samples yet discussed, substrate temperature is held constant throughout growth, that is, "one-step" samples. In "two-step" growth, NWs are first nucleated for a short time at a given temperature, then the substrate temperature is rapidly increased for the remainder of growth. The N shutter is left open while the temperature is ramped up (~1 min) to limit decomposition of the existing islands. This higher temperature is chosen to correspond with conditions at which NW nucleation is unlikely based on the growth phase diagram (Figure 2).

A series of samples illustrates the differences between NWs produced using the one-step or two-step method (Figure 3). For all samples the III/V flux ratio is 0.26. First, NWs are nucleated for 22.5 min at 765 °C. Samples grown under these conditions generate a density of 10−20 μm^{-2}. A one-step sample grown for a total time of 90 min is shown in Figure 3a, demonstrating that during the additional 67.5 min of growth after the nucleation step many more wires have nucleated. In contrast, if after the nucleation step the sample is ramped up to 780 °C and grown for an additional 67.5 min (total growth time = 90 min), the original density is maintained (Figure 3b). To more carefully examine the effect of the two-step growth method on the NW characteristics, six additional samples are prepared (Figure 3c−f). At short times (<30 min.), one-step samples show a low density consistent with the growth phase diagram (Figure 2), but at longer times, there is an increase in density due to the continuous nucleation of new NWs after the first 22.5 min until the density saturates near 500 μm^{-2}. Though not reaching complete surface saturation, the density is within a factor of 2 of the saturation density of ~1000 μm^{-2}. In contrast, two-step samples exhibit little to no change in density after the nucleation step (22.5 min.). This can be understood from the growth phase diagram (Figure 2) since at 780 °C additional NW nucleation is suppressed due to thermal decomposition of GaN and Ga adatom desorption. Even though the increased temperature in the two-step samples prevents new NWs from forming (nucleation suppression), the existing

dx.doi.org/10.1021/nl104265u |*Nano Lett.* 2011, 11, 866–871

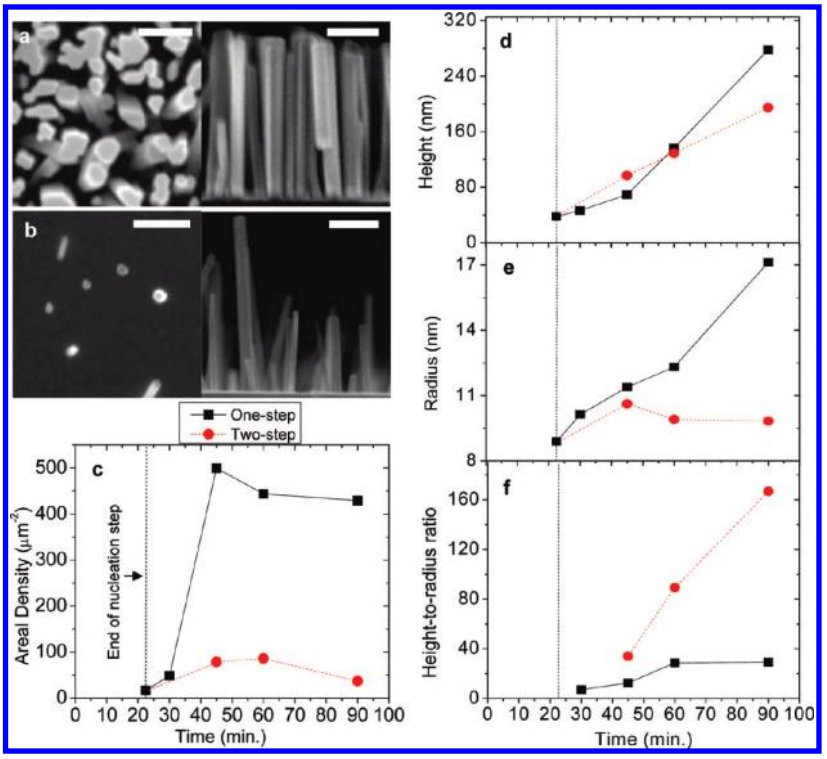

Figure 3. Comparison of GaN nanowire properties grown using one-step versus two-step process. Plan view (left) and cross-sectional view (right) SEM images of GaN nanowires grown using (a) the one-step method (765 °C for 90 min.), and (b) the two-step method (765 °C for 22.5 min, 780 °C for 67.5 min.). Scale bars correspond to 100 nm. (c) Nanowire areal density, (d) average height, (e) radius, and (f) height-to-radius ratio as a function of time. III/V = 0.26 for all samples. Lines guide the eye.

nanowires continue to grow (Figure 3d). As expected, the two-step sample growth rate is smaller than that of the the one-step samples precisely because two-step samples are grown well above the thermal decomposition temperature. It is worth noting that the growth rate in the two-step samples could also be increased by simultaneously increasing the III/V ratio in addition to the substrate temperature, although one must be careful to avoid nucleating additional NWs.

The two-step grown nanowires experience different growth kinetics and thus evolve differently from the one-step grown nanowires. This can clearly be seen by examining the difference in radial growth rate of the NWs between one-step and two-step samples (Figure 3e). Previous reports of GaN NWs are from one-step grown samples, and exhibit a vertical-to-radial growth rate ratio of approximately 30:1.[7,10,14] This value is relatively constant, providing a challenge for rational design of nanowire heterostructures since neither purely vertical nor purely coaxial heterostructures can be formed. In contrast, two-step GaN nanowires exhibit complete suppression of radial growth (Figure 3e), such that the vertical to radial growth rate ratio is no longer definable (diverges) (Figure 3f).

The suppression of radial growth in the two-step grown samples has two possible explanations. Either the change in growth kinetics alters the selective incorporation along *m*-plane (sidewalls) versus *c*-plane (tops), or the increased temperature leads to selective decomposition along the *m*-plane (sidewalls) versus the *c*-plane (tops). At higher temperatures, the Ga-adatom mobility should increase, leading to increased probability of adatoms reaching the more favorable *c*-plane sites on the tops. Determination of the mechanism for the suppression of radial growth will require additional work; however the current results clearly show elimination of radial growth of GaN nanowires resulting from the ability to access growth kinetics not possible using a traditional one-step growth process.

Arrays of three-dimensionally layered nanowire heterostructures of GaN/AlN can be formed using the two-step method. First, GaN NWs are grown at a target height (100 nm) and density (16 μm^{-2}) using a low-temperature nucleation step (765 °C, 22.5 min) followed by a high-temperature growth (780 °C, 67.5 min), then 50 periods of AlN and GaN are deposited on top of the NWs to form short period vertical superlattices (SLs) along the *c*-plane. The III/V ratio is held constant for both AlN and GaN depositions using flux measurement and calibration previously described. A low density of 16 μm^{-2} is chosen because in previous attempts at growing NW SLs (not shown here) the coalescence of NWs at higher density was a detriment to growing consistent NW SLs. Thus the two-step method provides a clear advantage in that a low density of nanowire heterostructures can be maintained over arbitrarily long growth times. High-resolution microscopy performed on an FEI Titan^3 80−300 probe-corrected monochromated scanning/transmission electron microscope (S/TEM) operated at 300 kV is displayed in Figure 4a. The microscope was operated in high-angle annular dark-field (HAADF) mode, providing Z-contrast. As expected (as in Figure 3e), radial deposition of GaN is not observed, only vertical deposition of GaN. In contrast, AlN forms both vertically and coaxially. The AlN vertical-coaxial growth rate ratio is estimated at 11:1, similar to reports from one-step grown GaN/AlN nanowires.[7] Layer thicknesses obtained from the Z-contrast images (inset) yield an average GaN layer thickness of 1.8 ± 0.2 nm corresponding to an average vertical growth rate of 2.8 ± 0.3 nm/min, which is larger than the value obtained in

dx.doi.org/10.1021/nl104265u |*Nano Lett.* 2011, 11, 866–871

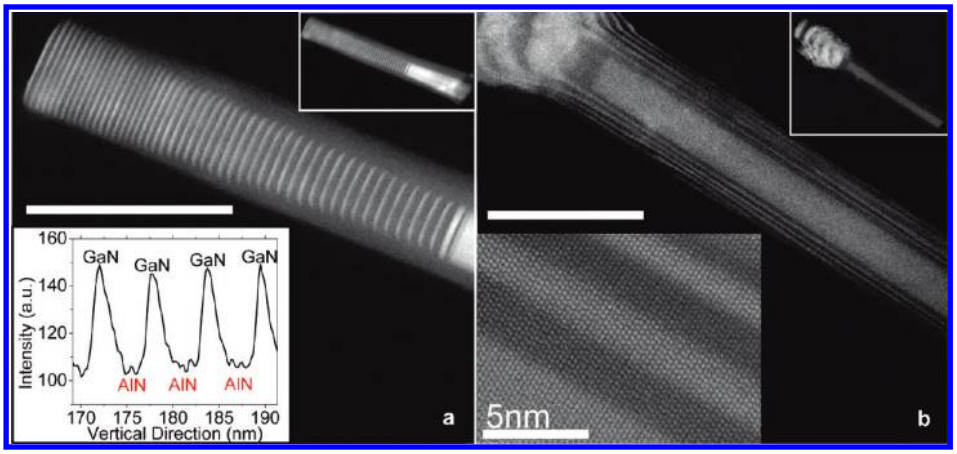

Figure 4. STEM images of three-dimensional GaN/AlN nanowire hetereostructures. (a) Fifty period vertically aligned AlN/GaN nanowire superlattice prepared using the two-step method. Top inset: zoomed out image of nanowire. Bottom inset: example of a profile intensity scan measuring compositional modulation along the nanowire's vertical *c*-axis direction. (b) Five period coaxially aligned AlN/GaN nanowire superlattice using the two-step procedure. Top inset: zoomed out image of nanowire. Bottom inset: section of coaxial layers imaged with atomic resolution. Dark (light) areas correspond to AlN (GaN) due to Z-contrast. All scale bars correspond to 100 nm unless labeled otherwise.

Figure 3d, 2.4 ± 0.1 nm/min, perhaps reflecting changes in the Ga adatom mobility on *m*-AlN versus *m*-GaN. Also, the GaN and AlN SL layer thicknesses decrease as the nanowire structure grows taller. This is because vertical growth rate is inversely proportional to nanowire diameter plus a constant[7] and AlN growing coaxially increases the nanowire's diameter throughout growth. Uniform heterostructures could be formed by adjusting the shutter time to compensate for this change in growth rate.

While vertical nanowire heterostructures were previously achieved using molecular beam epitaxy (MBE) or metalorganic chemical vapor deposition (MOCVD), the complete suppression of GaN coaxial growth using the two-step process is unique in that it allows the GaN quantum disks to be completely encased in high bandgap barrier material, AlN. This may prove useful for the development of vertical nanowire photonic and electronic devices. Optical studies of these enhanced multiple quantum disk structures will be the subject of a subsequent study.

Coaxially layered nanowire superlattices can also be formed using the dynamic growth method. First, GaN nanowires of a given density and height are formed in the two-step process by performing a low-temperature nucleation step (765 °C, 10 min) followed by a high-temperature growth (780 °C, 90 min). If the conditions were to remain the same from this point on, the nanowires would continue to grow vertically. Instead, the growth temperature is reduced to 500 °C and a five period superlattice of AlN and GaN is deposited. At 500 °C, adatom mobility is greatly reduced; Ga adatoms are less likely to reach the NW tops and simply incorporate into the NW *m*-plane sidewalls, Figure 4b (imaged under the same conditions as 4a). The coaxial layers for both GaN and AlN are about 1−2 nm. At higher magnification, atomically resolved images (inset) show that the interface between GaN and AlN coaxial layers are compositionally sharp within ±1 monolayer. While coaxial III-nitride nanowire heterostructures have been grown by chemical vapor deposition[26] and MOCVD[27,28] in the past, the MBE grown coaxial AlN/GaN SLs presented here are the first of their kind that exhibit atomically sharp compositional changes over monolayer distances and with multiple coaxial layers. The two-step process used to grow the GaN NW cores for this heterostructure is essential since a high density of nanowires would lead to shadowing of the impinging atomic beams. If the beams are shadowed then uneven coaxial layers will result. Thus establishing a low NW density with the two-step method is necessary for achieving uniform coaxial layers.

In conclusion, a growth phase diagram for catalyst-free GaN nanowires was developed allowing reproducible control of the density over three orders of magnitude. The effects of nucleation and growth were roughly separated using a two-step dynamic method allowing independent control of NW density and height. This allows access to growth kinetics at which the radial nanowire growth is eliminated for GaN as well as access to higher growth temperature for improved vertical nanowire heterostructure quality. Additionally, coaxial GaN/AlN superlattices were achieved by exploiting reduced adatom mobility at low temperatures. By separating the nucleation and growth process into distinct steps, growth kinetics can therefore be tuned to favor either vertical or radial growth, allowing design of three-dimensional nanowire heterostructures with monolayer precision, which may enable a variety of nanoelectronics and nanophotonics. In particular, nonpolar coaxial nanowire heterostructures allow flat band quantum structures that are shown to improve the efficiency of light-emitting diodes[29] by elimination of the polarization induced Stark shift. Additionally, intersubband-based devices would benefit from the coaxial confinement geometry since photons can be emitted or absorbed normal to the substrate surface.

AUTHOR INFORMATION

Corresponding Author

*E-mail: myers.1079@osu.edu.

ACKNOWLEDGMENT

We thank Professors Johnston-Halperin and S. Rajan and Drs. J. Grandal and A. Giussani for a critical reading of the manuscript and helpful comments. Technical support was provided by the Campus Electron Optics Facility and ENCOMM NanoSystems Laboratory. This work was supported by the ONR under Grant N00014-09-1-1153. Partial support was provided by The Ohio State University Institute for Materials Research.

REFERENCES

(1) Thillosen, N.; Sebald, K.; Hardtdegen, H.; Meijers, R.; Calarco, R.; Montanari, S.; Kaluza, N.; Gutowski, J.; Luth, H. The State of Strain in Single GaN Nanocolumns As Derived from Micro-Photoluminescence Measurements. *Nano Lett.* **2006**, *6*, 704–708.

(2) Guo, W.; Zhang, M.; Banerjee, A.; Bhattacharya, P. Catalyst-Free InGaN/GaN Nanowire Light Emitting Diodes Grown on (001) Silicon by Molecular Beam Epitaxy. *Nano Lett.* **2010**, *10*, 3355–3359.

(3) Lin, H.; Lu, Y.; Chen, H.; Lee, H.; Gwo, S. InGaN/GaN nanorod array white light-emitting diode. *Appl. Phys. Lett.* **2010**, *97*, No. 073101.

(4) Rigutti, L.; Tchernycheva, M.; Bugallo, A. D. L.; Jacopin, G.; Julien, F. H.; Zagonel, L. F.; March, K.; Stephan, O.; Kociak, M.; Songmuang, R. Ultraviolet Photodetector Based on GaN/AlN Quantum Disks in a Single Nanowire. *Nano Lett.* **2010**, *10*, 2939–2943.

(5) Kikuchi, A.; Kawai, M.; Tada, M.; Kishino, K. InGaN/GaN multiple quantum disk nanocolumn light-emitting diodes grown on (111)Si substrate. *Jpn. J. Appl. Phys., Part 2* **2004**, *43*, L1524–L1526.

(6) Ristic, J.; Calleja, E.; Fernandez-Garrido, S.; Cerutti, L.; Trampert, A.; Jahn, U.; Ploog, K. H. On the mechanisms of spontaneous growth of III-nitride nanocolumns by plasma-assisted molecular beam epitaxy. *J. Cryst. Growth* **2008**, *310*, 4035–4045.

(7) Calarco, R.; Meijers, R. J.; Debnath, R. K.; Stoica, T.; Sutter, E.; Luth, H. Nucleation and Growth of GaN Nanowires on Si(111) Performed by Molecular Beam Epitaxy. *Nano Lett.* **2007**, *7*, 2248–2251.

(8) Yamashita, T.; Hasegawa, S.; Nishida, S.; Ishimaru, M.; Hirotsu, Y.; Asahi, H. Electron field emission from GaN nanorod films grown on Si substrates with native silicon oxides. *Appl. Phys. Lett.* **2005**, *86*, No. 082109.

(9) Park, Y. S.; Lee, S. H.; Oh, J. E.; Park, C. M.; Kang, T. W. Self-assembled GaN nano-rods grown directly on (111) Si substrates: Dependence on growth conditions. *J. Cryst. Growth* **2005**, *282*, 313–319.

(10) Songmuang, R.; Landre, O.; Daudin, B. From nucleation to growth of catalyst-free GaN nanowires on thin AlN buffer layer. *Appl. Phys. Lett.* **2007**, *91*, No. 251902.

(11) Consonni, V.; Knelangen, M.; Geelhaar, L.; Trampert, A.; Riechert, H. Nucleation mechanisms of epitaxial GaN nanowires: Origin of their self-induced formation and initial radius. *Phys. Rev. B* **2010**, *81*, No. 085310.

(12) Bertness, K. A.; Roshko, A.; Mansfield, L. M.; Harvey, T. E.; Sanford, N. A. Nucleation conditions for catalyst-free GaN nanowires. *J. Cryst. Growth* **2007**, *300*, 94–99.

(13) Meijers, R.; Richter, T.; Calarco, R.; Stoica, T.; Bochem, H. P.; Marso, M.; Luth, H. GaN-nanowhiskers: MBE-growth conditions and optical properties. *J. Cryst. Growth* **2006**, *289*, 381–386.

(14) Tchernycheva, M.; Sartel, C.; Cirlin, G.; Travers, L.; Patriarche, G.; Harmand, J.; Dang, L. S.; Renard, J.; Gayral, B.; Nevou, L.; Julien, F. Growth of GaN free-standing nanowires by plasma-assisted molecular beam epitaxy: structural and optical characterization. *Nanotechnology* **2007**, *18*, No. 385306.

(15) Debnath, R. K.; Meijers, R.; Richter, T.; Stoica, T.; Calarco, R.; Lueth, H. Mechanism of molecular beam epitaxy growth of GaN nanowires on Si(111). *Appl. Phys. Lett.* **2007**, *90*, No. 123117.

(16) Bertness, K. A.; Sanford, N. A.; Barker, J. M.; Schlager, J. B.; Roshko, A.; Davydov, A. V.; Levin, I. Catalyst-free growth of GaN nanowires. *J. Electron. Mater.* **2006**, *35*, 576–580.

(17) Hsiao, C. L.; Tu, L. W.; Chi, T. W.; Seo, H. W.; Chen, Q. Y.; Chu, W. K. Buffer controlled GaN nanorods growth on Si(111) substrates by plasma-assisted molecular beam epitaxy. *J. Vac. Sci. Technol., B* **2006**, *24*, 845–851.

(18) Bertness, K. A.; Roshko, A.; Sanford, N. A.; Barker, J. M.; Davydov, A. Spontaneously grown GaN and AlGaN nanowires. *J. Cryst. Growth* **2006**, *287*, 522–527.

(19) Nath, D. N.; Gur, E.; Ringel, S. A.; Rajan, S. Molecular beam epitaxy of N-polar InGaN. *Appl. Phys. Lett.* **2010**, *97*, No. 071903.

(20) Fukaya, Y.; Shigeta, Y. New phase and surface melting of Si(111) at high temperature above the (7×7)-(1×1) phase transition. *Phys. Rev. Lett.* **2000**, *85*, 5150–5153.

(21) Ishizaka, A.; Doi, T.; Ichikawa, M. Possibility of a New Phase-Transition in 7 X 7 Structure on Clean Si(111) Surfaces. *Appl. Phys. Lett.* **1991**, *58*, 902–904.

(22) Heying, B.; Averbeck, R.; Chen, L. F.; Haus, E.; Riechert, H.; Speck, J. S. Control of GaN surface morphologies using plasma-assisted molecular beam epitaxy. *J. Appl. Phys.* **2000**, *88*, 1855–1860.

(23) Abramoff, M. D.; Magelhaes, P. J.; Ram, S. J. Image Processing with ImageJ. *Biophotonics International* **2004**, *11*, 36.

(24) Grandjean, N.; Massies, J.; Semond, F.; Karpov, S. Y.; Talalaev, R. A. GaN evaporation in molecular-beam epitaxy environment. *Appl. Phys. Lett.* **1999**, *74*, 1854–1856.

(25) Ptak, A. J.; Millecchia, M. R.; Myers, T. H.; Ziemer, K. S.; Stinespring, C. D. The relation of active nitrogen species to high-temperature limitations for (000(1)over-bar) GaN growth by radio-frequency-plasma-assisted molecular beam epitaxy. *Appl. Phys. Lett.* **1999**, *74*, 3836–3838.

(26) Choi, H. J.; Johnson, J. C.; He, R. R.; Lee, S. K.; Kim, F.; Pauzauskie, P.; Goldberger, J.; Saykally, R. J.; Yang, P. D. Self-Organized GaN Quantum Wire UV Lasers. *J. Phys. Chem. B* **2003**, *107*, 8721–8725.

(27) Dong, Y. J.; Tian, B. Z.; Kempa, T. J.; Lieber, C. M. Coaxial Group III-Nitride Nanowire Photovoltaics. *Nano Lett.* **2009**, *9*, 2183–2187.

(28) Qian, F.; Gradecak, S.; Li, Y.; Wen, C. Y.; Lieber, C. M. Core/multishell nanowire heterostructures as multicolor, high-efficiency light-emitting diodes. *Nano Lett.* **2005**, *5*, 2287–2291.

(29) Paskova, T. Development and prospects of nitride materials and devices with nonpolar surfaces. *Phys. Status Solidi B* **2008**, *245*, 1011–1025.